Attosecond dispersion control by extreme ultraviolet multilayer mirrors

Michael Hofstetter,[1,2,*] Martin Schultze,[1,2] Markus Fieß,[2] Benjamin Dennhardt,[2,3] Alexander Guggenmos,[1,2] Justin Gagnon,[1,2] Vladislav S. Yakovlev,[1,2] Eleftherios Goulielmakis,[2] Reinhard Kienberger,[2,3] Eric M. Gullikson,[4] Ferenc Krausz,[1,2] and Ulf Kleineberg[1,2]

[1]*Ludwig-Maximilians-Universität München, Fakultät für Physik, Am Coulombwall 1, D-85748 Garching, Germany*
[2]*Max Planck Institut für Quantenoptik, Hans-Kopfermann-Str. 1, D-85748 Garching, Germany*
[3]*Technische Universität München, Physik Department E11, James-Franck-Straße, D-85748 Garching, Germany*
[4]*Center for X-Ray Optics, Lawrence Berkeley National Lab 2-400, Berkeley, California 94720 USA*
** michael.hofstetter@mpq.mpg.de*

Abstract: We report the first experimental demonstration of a-periodic multilayer mirrors controlling the frequency sweep (chirp) of isolated attosecond *XUV* pulses. The concept was proven with about 200-attosecond pulses in the photon energy range of 100-130 *eV* measured via photoelectron streaking in neon. The demonstrated attosecond dispersion control is engineerable in a wide range of *XUV* photon energies and bandwidths. The resultant tailor-made attosecond pulses with highly enhanced photon flux are expected to significantly advance attosecond metrology and spectroscopy and broaden their range of applications.

OCIS codes: (320.0320) Ultrafast optics; (320.1590) Chirping; (320.5540) Pulse shaping; (340.7480) X-rays, soft x-rays, extreme ultraviolet (EUV); (310.4165) Multilayer design.

References and links

1. M. Drescher, M. Hentschel, R. Kienberger, G. Tempea, C. Spielmann, G. A. Reider, P. B. Corkum, and F. Krausz, "X-ray pulses approaching the attosecond frontier," Science **291**(5510), 1923–1927 (2001).
2. A. L. Cavalieri, N. Müller, T. Uphues, V. S. Yakovlev, A. Baltuška, B. Horvath, B. Schmidt, L. Blümel, R. Holzwarth, S. Hendel, M. Drescher, U. Kleineberg, P. M. Echenique, R. Kienberger, F. Krausz, and U. Heinzmann, "Attosecond spectroscopy in condensed matter," Nature **449**(7165), 1029–1032 (2007).
3. M. Uiberacker, Th. Uphues, M. Schultze, A. J. Verhoef, V. Yakovlev, M. F. Kling, J. Rauschenberger, N. M. Kabachnik, H. Schröder, M. Lezius, K. L. Kompa, H.-G. Muller, M. J. J. Vrakking, S. Hendel, U. Kleineberg, U. Heinzmann, M. Drescher, and F. Krausz, "Attosecond real-time observation of electron tunnelling in atoms," Nature **446**(7136), 627–632 (2007).
4. M. Schultze, M. Fieß, N. Karpowicz, J. Gagnon, M. Korbman, M. Hofstetter, S. Neppl, A. L. Cavalieri, Y. Komninos, Th. Mercouris, C. A. Nicolaides, R. Pazourek, S. Nagele, J. Feist, J. Burgdörfer, A. M. Azzeer, R. Ernstorfer, R. Kienberger, U. Kleineberg, E. Goulielmakis, F. Krausz, and V. S. Yakovlev, "Delay in photoemission," Science **328**(5986), 1658–1662 (2010).
5. E. Goulielmakis, Z. H. Loh, A. Wirth, R. Santra, N. Rohringer, V. S. Yakovlev, S. Zherebtsov, T. Pfeifer, A. M. Azzeer, M. F. Kling, S. R. Leone, and F. Krausz, "Real-time observation of valence electron motion," Nature **466**(7307), 739–743 (2010).
6. A. Wonisch, U. Neuhäusler, N. M. Kabachnik, T. Uphues, M. Uiberacker, V. Yakovlev, F. Krausz, M. Drescher, U. Kleineberg, and U. Heinzmann, "Design, fabrication, and analysis of chirped multilayer mirrors for reflection of extreme-ultraviolet attosecond pulses," Appl. Opt. **45**(17), 4147–4156 (2006).
7. A.-S. Morlens, P. Balcou, P. Zeitoun, C. Valentin, V. Laude, and S. Kazamias, "Compression of attosecond harmonic pulses by extreme-ultraviolet chirped mirrors," Opt. Lett. **30**(12), 1554–1556 (2005).
8. M. Suman, G. Monaco, M.-G. Pelizzo, D. L. Windt, and P. Nicolosi, "Realization and characterization of an XUV multilayer coating for attosecond pulses," Opt. Express **17**(10), 7922–7932 (2009).
9. M. Hentschel, R. Kienberger, Ch. Spielmann, G. A. Reider, N. Milosevic, T. Brabec, P. Corkum, U. Heinzmann, M. Drescher, and F. Krausz, "Attosecond metrology," Nature **414**(6863), 509–513 (2001).
10. I. P. Christov, M. M. Murnane, and H. C. Kapteyn, "High-Harmonic Generation of Attosecond Pulses in the "Single-Cycle" Regime," Phys. Rev. Lett. **78**(7), 1251–1254 (1997).
11. R. Kienberger, E. Goulielmakis, M. Uiberacker, A. Baltuška, V. Yakovlev, F. Bammer, A. Scrinzi, Th. Westerwalbesloh, U. Kleineberg, U. Heinzmann, M. Drescher, and F. Krausz, "Atomic transient recorder," Nature **427**(6977), 817–821 (2004).
12. F. Krausz, and M. Ivanov, "Attosecond physics," Rev. Mod. Phys. **81**(1), 163–234 (2009).

#138629 - $15.00 USD Received 23 Nov 2010; revised 31 Dec 2010; accepted 3 Jan 2011; published 14 Jan 2011

13. E. Goulielmakis, M. Uiberacker, R. Kienberger, A. Baltuška, V. Yakovlev, A. Scrinzi, Th. Westerwalbesloh, U. Kleineberg, U. Heinzmann, M. Drescher, and F. Krausz, "Direct measurement of light waves," Science **305**(5688), 1267–1269 (2004).
14. V. Pervak, A. V. Tikhonravov, M. K. Trubetskov, S. Naumov, F. Krausz, and A. Apolonski, "1.5-octave chirped mirror for pulse compression down to sub-3 fs," Appl. Phys. B **87**(1), 5–12 (2007).
15. E. Gustafsson, T. Ruchon, M. Swoboda, T. Remetter, E. Pourtal, R. López-Martens, Ph. Balcou, and A. L'Huillier, "Broadband attosecond pulse shaping," Opt. Lett. **32**(11), 1353–1355 (2007).
16. R. López-Martens, K. Varjú, P. Johnsson, J. Mauritsson, Y. Mairesse, P. Salières, M. B. Gaarde, K. J. Schafer, A. Persson, S. Svanberg, C.-G. Wahlström, and A. L'huillier, "Amplitude and phase control of attosecond light pulses," Phys. Rev. Lett. **94**(3), 033001 (2005).
17. G. Sansone, E. Benedetti, F. Calegari, C. Vozzi, L. Avaldi, R. Flammini, L. Poletto, P. Villoresi, C. Altucci, R. Velotta, S. Stagira, S. De Silvestri, and M. Nisoli, "Isolated single-cycle attosecond pulses," Science **314**(5798), 443–446 (2006).
18. E. Goulielmakis, M. Schultze, M. Hofstetter, V. S. Yakovlev, J. Gagnon, M. Uiberacker, A. L. Aquila, E. M. Gullikson, D. T. Attwood, R. Kienberger, F. Krausz, and U. Kleineberg, "Single-cycle nonlinear optics," Science **320**(5883), 1614–1617 (2008).
19. M. Drescher, M. Hentschel, R. Kienberger, M. Uiberacker, V. Yakovlev, A. Scrinzi, Th. Westerwalbesloh, U. Kleineberg, U. Heinzmann, and F. Krausz, "Time-resolved atomic inner-shell spectroscopy," Nature **419**(6909), 803–807 (2002).
20. Y. Ménesguen, S. de Rossi, E. Meltchakov, and F. Delmotte, "Aperiodic multilayer mirrors for efficient broadband reflection in the extreme ultraviolet," Appl. Phys., A Mater. Sci. Process. **98**(2), 305–309 (2010).
21. M. Hofstetter, M. Schultze, M. Fieß, A. Guggenmos, J. Gagnon, E. Magerl, E. Botschafter, R. Ernstorfer, R. Kienberger, E. M. Gullikson, F. Krausz, and U. Kleineberg, "First attosecond pulse control by multilayer mirrors above 100 eV photon energy," in *Ultrafast Phenomena XVII*, 11.17, M. Chergui, D. Jonas, E. Riedle, B. Schönlein, A. Taylor (Oxford University Press, New York, 2010).
22. A. V. Tikhonravov, M. K. Trubetskov, and G. W. DeBell, "Optical coating design approaches based on the needle optimization technique," Appl. Opt. **46**(5), 704–710 (2007).
23. B. L. Henke, E. M. Gullikson, and J. C. Davis, "X-ray interactions: photoabsorption, scattering, transmission, and reflection at E=50-30000 eV, Z=1-92," At. Data Nucl. Data Tables **54**(2), 181–342 (1993).
24. E. M. Gullikson, J. H. Underwood, P. Batson, and V. Nikitin, "A soft x-ray/EUV reflectometer based on a laser produced plasma source," J. XRay Sci. Technol. **3**(4), 283–299 (1992).
25. A. Aquila, F. Salmassi, and E. Gullikson, "Metrologies for the phase characterization of attosecond extreme ultraviolet optics," Opt. Lett. **33**(5), 455–457 (2008).
26. M. Kitzler, N. Milosevic, A. Scrinzi, F. Krausz, and T. Brabec, "Quantum theory of attosecond XUV pulse measurement by laser dressed photoionization," Phys. Rev. Lett. **88**(17), 173904 (2002).
27. R. Kienberger, M. Hentschel, M. Uiberacker, Ch. Spielmann, M. Kitzler, A. Scrinzi, M. Wieland, Th. Westerwalbesloh, U. Kleineberg, U. Heinzmann, M. Drescher, and F. Krausz, "Steering attosecond electron wave packets with light," Science **297**(5584), 1144–1148 (2002).
28. M. Schultze, E. Goulielmakis, M. Uiberacker, M. Hofstetter, J. Kim, D. Kim, F. Krausz, and U. Kleineberg, "Powerful 170-attosecond XUV pulses generated with few-cycle laser pulses and broadband multilayer optics," N. J. Phys. **9**(7), 243 (2007).
29. M. Fieß, M. Schultze, E. Goulielmakis, B. Dennhardt, J. Gagnon, M. Hofstetter, R. Kienberger, and F. Krausz, "Versatile apparatus for attosecond metrology and spectroscopy," Rev. Sci. Instrum. **81**, 1 (2010).
30. R. Trebino, K. W. DeLong, D. N. Fittinghoff, J. N. Sweetser, M. A. Krumbügel, B. A. Richman, and D. J. Kane, "Measuring ultrashort laser pulses in the time-frequency domain using frequency-resolved optical gating," Rev. Sci. Instrum. **68**(9), 3277 (1997).
31. A download link of the program can be found at http://www.attoworld.de/Home/ourResearch/Downloads/index.html
32. Y. Mairesse, A. de Bohan, L. J. Frasinski, H. Merdji, L. C. Dinu, P. Monchicourt, P. Breger, M. Kovačev, R. Taïeb, B. Carré, H. G. Muller, P. Agostini, and P. Salières, "Attosecond synchronization of high-harmonic soft x-rays," Science **302**(5650), 1540–1543 (2003).
33. J. Gagnon, E. Goulielmakis, and V. S. Yakovlev, "The accurate FROG characterization of attosecond pulses from streaking measurements," Appl. Phys. B **92**(1), 25–32 (2008).
34. J. Gagnon, and V. S. Yakovlev, "The robustness of attosecond streaking measurements," Opt. Express **17**(20), 17678–17693 (2009).
35. L. Y. Peng, F. Tan, Q. Gong, E. A. Pronin, and A. F. Starace, "Few-cycle attosecond pulse chirp effects on asymmetries in ionized electron momentum distributions," Phys. Rev. A **80**(1), 013407 (2009).
36. V. S. Yakovlev, J. Gagnon, N. Karpowicz, and F. Krausz, "Attosecond streaking enables the measurement of quantum phase," Phys. Rev. Lett. **105**(7), 073001 (2010).
37. Y. Li, J. Lewellen, Z. Huang, V. Sajaev, and S. V. Milton, "Time-resolved measurement of a self-amplified free-electron laser," NIM A **507**(1-2), 413–416 (2003).

1. Introduction

Attosecond (1 *as* = 10^{-18} *s*) light pulses at short wavelength from the extreme ultraviolet (*XUV*) to the soft *X*-ray regime have recently gained fundamental importance in studying electron motions in atoms, molecules or at surfaces [1–5]. Here, fundamental ultrafast

#138629 - $15.00 USD Received 23 Nov 2010; revised 31 Dec 2010; accepted 3 Jan 2011; published 14 Jan 2011

electron dynamics in excitation, transport and emission processes on time scales of a few tens of attoseconds can be observed. These ultrashort time-scales of electron motion are inevitably connected to atomic or mesoscopic spatial scales and nano-scaled microscopic resolution can be provided by the short wavelength nature of the soft *X*-ray pulses itself. The performance and applicability of attosecond spectroscopy critically depends on the flux, photon energy, bandwidth and dispersion control of attosecond pulses. Multilayer-coated *XUV* mirrors [6–8] have served attosecond metrology from its very beginning [9], by focusing and isolating single attosecond pulses from coherent high-order harmonic radiation [10–13]. Chirped multilayer mirrors in the visible/infrared range, are inevitable components in generating few cycle laser pulses of a few femtosecond pulse-length only. Those are the necessary driving pulses for attosecond pulse generation [14]. In contrast to the development of chirped dielectric mirrors in the visible, the realization of chirped *XUV* multilayer mirrors requires new approaches in computational design, manufacturing and characterization, which have not been available and combined until now. So far, *XUV* dispersion control over multi-electron volt bandwidths could only be accomplished for photon energies below 100 *eV* [15–19]. Further, control of the spectral distribution and chirp of an attosecond extreme ultraviolet pulse have so far been realized by means of ultrathin metal filters (typical thickness ~100 *nm*) [15–17] and *XUV* multilayer mirrors [18,19] with chirp control mainly relying on the metal filter components. Their applicability is limited due to strong *XUV* attenuation and the availability of only few materials, thus only specific spectral ranges, where the real part of the complex index of refraction provides sufficient (usually only negative) dispersion.

Specially designed non-periodic binary or ternary multilayer-coated *XUV* mirrors allow for a large degree of freedom in influencing the *XUV* pulse characteristics by reflection of those mirrors [20,21]. So far, multilayer mirrors in attosecond physics applications were used as band-pass reflectors preserving the spectral phase of the attosecond pulse that is defined in the generation process and by the dispersion characteristics of all *XUV* optical elements passed by the pulse. In this work we demonstrate, how specially designed non-periodic multilayer *XUV* mirrors furnish attosecond technology with the ability to control the spectral phase in addition to spectral intensity of attosecond pulses, offering a great degree of freedom in influencing the *XUV* pulse characteristics, such as the pulse shape, duration, frequency sweep and central wavelength.

2. The Experiment

2.1 Concept

Within this paper, the group delay (*GD*) τ is defined as the *negative* derivative of the spectral phase $\phi(\omega)$ with respect to angular frequency ω, $\tau = -d\phi/d\omega$. Its derivative is the group delay dispersion $GDD = d\tau/d\omega$, known to be the lowest order phase term that temporally broadens the pulse.

Figure 1 displays a computational example for group-delay dispersion (*GDD*) management by non-periodic multilayer coatings optimized to introduce positive (left panel) or negative (right panel) *GDD* to an initially unchirped *XUV* pulse (higher order dispersion control like third order dispersion *TOD* by non-periodic multilayer is also feasible, although not demonstrated here). The square of the electric field amplitude of the standing wave resulting from the superposition of the incident and reflected radiation depicted by the false-colour plots reveals a penetration depth varying nearly linearly with photon energy in the centre of the high-reflectivity (*HR*) range of the multilayer Bragg peak (≈ 100-130 *eV*). The penetration depth increasing and decreasing with photon energy imposes a positive and negative chirp, respectively, on an originally bandwidth-limited attosecond pulse reflected by the mirror. Thus, introducing positive *GDD* results in a positive chirp of an initially unchirped pulse and vice versa.

#138629 - $15.00 USD Received 23 Nov 2010; revised 31 Dec 2010; accepted 3 Jan 2011; published 14 Jan 2011

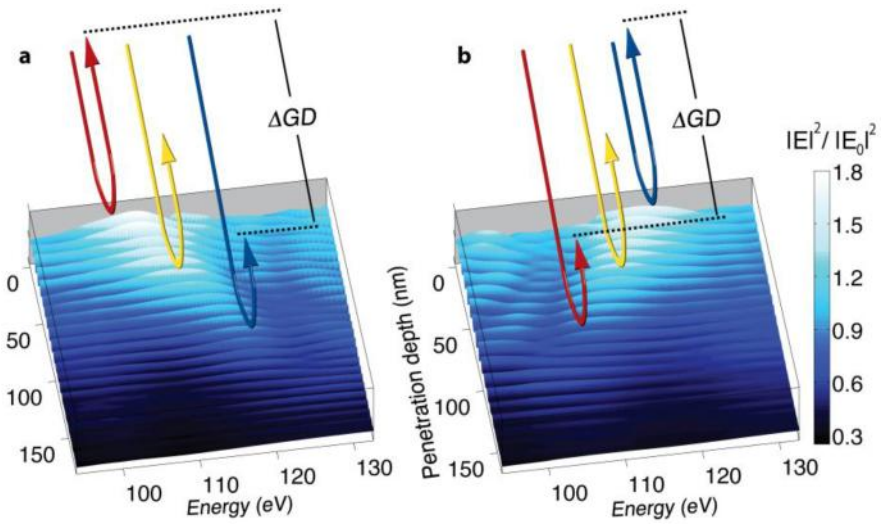

Fig. 1. Operational principle of *XUV* chirped multilayers: Calculated square of the electric field amplitude of the standing wave formed in the multilayer structure upon reflection in the 94–133 *eV* photon energy range, normalized to that of the incident wave. Following the energy dependent maxima of the standing field, it is obvious that the penetration depth is wavelength dependent. Thus the mirrors introduce positive (a) and negative (b) chirp, resulting in an increasing and decreasing group delay for increasing photon energy respectively as the energy-dependent penetration depth signifies as depicted by the coloured arrows. The multilayer structure assumed here resembles the experimentally realized a-periodic multilayer mirrors as displayed in Fig. 2 (a/d) and (c/f).

2.2 Design

To prove the validity of the concept for precision chirp control of attosecond *XUV* pulses, we have developed a set of three multilayer mirrors exhibiting distinctly different *GDD* but similar reflectivity characteristics. Optimized for an incident angle of 45° they exhibit high reflectivity within the range of 100-130 *eV* with comparable full widths at half maximum energy bandwidth: ΔE = 11-13 *eV FWHM* and peaking at different central energies within the range of 107-122 *eV*.

The multilayer designs have been calculated and optimized by a Fresnel equation thin film code coupled to a needle optimization algorithm [22]. The mirrors have been designed such, that the *GDD* is almost maximum and mostly linear within the final attosecond pulse spectrum. Small shifts of the mirror spectrum due to the thin metal filter or the shape of the high harmonic cut-off spectrum have been estimated and taken into account in the design. The calculated designs have been optimized for additional suppressed reflectivity contributions in the near vicinity of the main Bragg peak and have been tested for stability against small layer thickness deviations. *X*-ray optical constants in the *XUV* are based on the tabulated data of Henke and Gullikson [23]. The final multilayer coating designs are displayed in the lower panels (*d-f*) of Fig. 2. While the designs of the positively- and the negatively-chirped mirrors contain around 30 layers *Mo*/B_4C the almost unchirped mirror is a 17 layer *Mo*/*Si*/B_4C stack. The mirrors have been deposited by means of Dual Ion Beam Deposition (*DIBD*) on flat high-polished glass substrates. Interface losses and compound formation have been included in the calculation and could be compensated within the coating procedure.

#138629 - $15.00 USD Received 23 Nov 2010; revised 31 Dec 2010; accepted 3 Jan 2011; published 14 Jan 2011

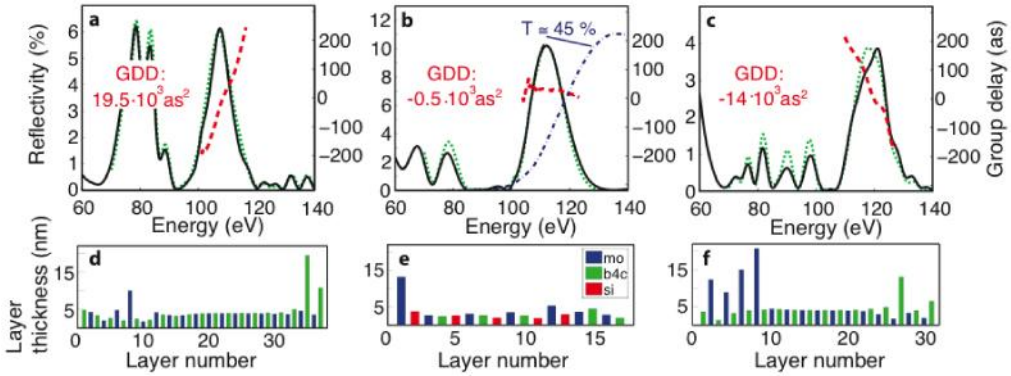

Fig. 2. Characteristics of *XUV* chirped multilayer coatings designed and manufactured for the experiments: Set of *XUV* multilayers with positive (a), near zero (b) and negative (c) group delay dispersion. The diagrams compare the measured (solid black) with the designed (dotted green) reflectivity curves. The calculated group delays (derivative of the spectral phase with respect to angular frequency) are also displayed (dashed red curve). The transmittivity of a 150-nm palladium foil is additionally qualitatively plotted in panel (b), depicted by the blue dash-dotted line. The lower panels (d), (e) and (f) show the corresponding mirror-designs of the appropriate mirrors above. Each colour represents one material as explained by the legend in 2(e).

Figure 2(a)–2(c) shows the calculated reflectivity and group delay of the three multilayer mirrors versus photon energy, compared with the reflectivity measured by *X*-ray reflectometry using synchrotron radiation [24]. The measured and computed *XUV* reflectivities are in excellent agreement, revealing maximum peak reflectivities between 4 and 10 percent. Notable deviations in the peak shape appear only in Fig. 2(c) near 120 *eV*, possibly due to minor uncertainties in the deposition layer thicknesses. In our proof-of-concept experiments, radiation at photon energies below 100 *eV* is suppressed by a 150 *nm* thick Palladium (*Pd*) filter (its transmittivity is shown in Fig. 2(b) by the blue dash-dotted line). The throughput of this high-pass filter combination could be enhanced by fine-tuning the filter thickness and the mirrors' high-reflectivity band. Since isolated attosecond pulses can be extracted by spectral filtering from the cut-off part of the generated *HH* spectrum [9], the high energy extend of the spectrum has to coincide with the high reflectivity range of the mirror. Reflectivity above this energy window thus does not affect the attosecond pulse generation. The three mirrors are designed to introduce substantial positive *GDD*, negligible *GDD*, and substantial negative *GDD*, with computed values of $19.5\text{x}10^3$ as^2, $-0.5\text{x}10^3$ as^2, and $-14\text{x}10^3$ as^2, respectively.

2.3 Streaking spectrograms and analyses

In contrast to the reflectivity, there is no standard frequency-domain technique available for measuring *GDD* in the extreme ultraviolet spectral range. Aquila *et. al.* have characterized the *GDD* of a multilayer mirror by measuring the photoelectron yield from its surface [25]. Here we have resorted to attosecond metrology for measuring the attosecond pulse dispersion directly and assessing the mirrors' capability of controlling the chirp of isolated attosecond *XUV* pulses [12,15,26].

Unlike in the well known collinear setup [27,28], where a concentric double mirror is used to introduce a delay between the inner (lower divergent) *XUV* beam and the outer (higher divergent) laser beam, in our setup the laser and *XUV* beam are completely spatially separated in two paths of an interferometric setup before recollimation [29]. Thus focusing of the *XUV* radiation (by means of a grazing incidence parabola) and time delay introduction between the *XUV* and the laser pulse (by means of a delay stage in the optical beam path) is decoupled from the plane *XUV* multilayer mirror. This technique allows for an easy and rapid exchange and alignment of the 45 *deg XUV* mirrors, which is inevitable for future *XUV* phase sensitive attosecond experiments.

#138629 - $15.00 USD Received 23 Nov 2010; revised 31 Dec 2010; accepted 3 Jan 2011; published 14 Jan 2011

We have implemented attosecond streaking by liberating photoelectrons from the *2p* sub-shell of an ensemble of neon atoms with sub-300-attosecond *XUV* pulses filtered by the combination of a *Pd* foil and one of the band-pass multilayer mirrors described above. The energy distribution of the ejected electrons has been streaked by the controlled linearly polarized electric field of near-single-cycle near-infrared (*NIR*) laser pulses [11,18,26]. The streaked spectra for electrons collected in a narrow cone aligned with the laser polarization were recorded as a function of the delay between the ionizing *XUV* pulse and the streaking *NIR* field.

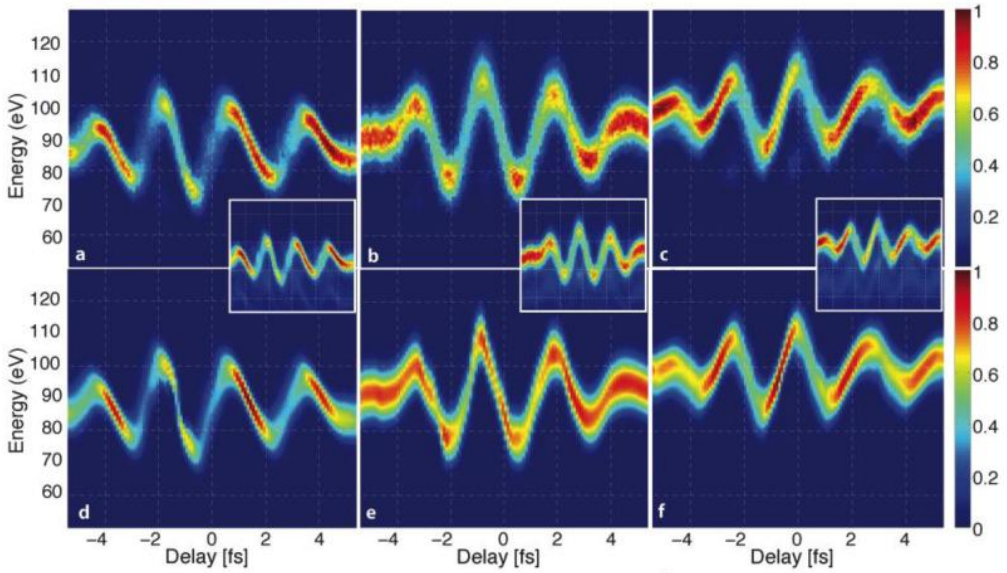

Fig. 3. Measured and retrieved attosecond electron streaking spectrograms, upper and lower row, respectively. Panels (a)-(c) and (d)-(f) display spectrograms recorded with attosecond pulses reflected off the mirrors described in Fig. 2(a)–2(c), respectively. The energy shift in the recorded spectra is proportional to the vector potential $A_L(t)$ of the streaking laser field at the instant of photoemission, hence the dependence of this energy shift on the delay between the attosecond *XUV* pulse and the *NIR* laser field reflects the temporal evolution of the *NIR* laser field's vector potential, $A_L(t)$. Narrowing and broadening in the streaked electron spectra at the zero crossings is displayed by enhanced and diminished electron count rates, respectively. The small insets show the energy calibrated raw data before subtraction of the background.

To access the temporal intensity profile of the synthesized attosecond pulses and their frequency sweep we performed a frequency-resolved optical gating (*FROG*) analysis [30,31] of the acquired streaking spectrograms. This method gives not only access to a full characterization of the laser vector potential, it allows us as well to characterize the spectral intensity distribution and the group delay variation [32,33] of the final attosecond *XUV* pulse reflected from the mirrors after passing the filter, allowing for a direct comparison of its *GDD* with the design values of the mirrors' *GDD*. The resultant streaking spectrograms recorded with the three mirrors of Fig. 2(a)–2(c) are displayed in Fig. 3(a)–3(c) along with their corresponding *FROG* retrievals in Fig. 3(d)–3(f), respectively. The streaked energy spectra of electrons ejected from the *2p* sub-shell are accompanied by a low- energy background originating from various processes, including inelastic scattering, above-threshold ionization via the *NIR* field, contribution from a small satellite pulse and shakeup channels. The *2p* spectrogram also slightly overlaps with that corresponding to *2s* electrons. We subtracted this undesirable background in order to isolate the *2p* spectrogram for a *FROG* analysis. The insets in Fig. 3 show the raw data before subtraction of that background. All features of the spectrograms remain obviously untouched. Thus the choice of the background function does not affect the qualitative result but has some influence on the details of the quantitative

#138629 - $15.00 USD Received 23 Nov 2010; revised 31 Dec 2010; accepted 3 Jan 2011; published 14 Jan 2011

analyses. Using the *FROG CRAB* algorithm *Attogram* described in refs [33,34], we retrieved the vector potential of the streaking *NIR* laser field together with the spectral phase and intensity distribution of the attosecond *XUV* pulse. Figure 3(d)–3(f) depict the corresponding streaking spectrograms calculated from the retrieved *NIR* waveform and *XUV* pulse. The calculated spectrograms appear to be in excellent agreement with the measured ones.

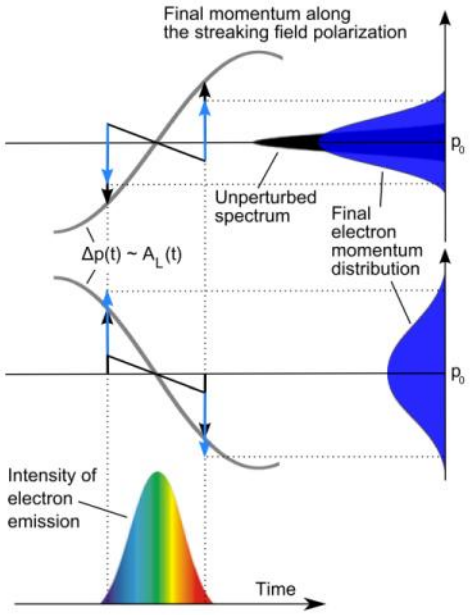

Fig. 4. Qualitative analysis of attosecond streak images of a linearly negatively-chirped attosecond pulse. For explanation, see text.

The spectrograms clearly reveal signatures of the chirp imposed to the *XUV* pulse after being reflected by the chirped *XUV* multilayer mirrors. In order to recognize these signatures, we analyse, with the help of Fig. 4, qualitatively the implications of lowest-order (linear) frequency sweep of the attosecond *XUV* pulse on its streaking spectrogram recorded with a linearly polarized few-cycle field. The linear chirp causes a linear sweep of initial photoelectron momenta depicted by the slanted black straight lines in Fig. 4. The laser field transfers a momentum Δp to the *XUV*-released electron that is proportional to the vector potential $A_L(t)$ of the streaking field at the instant of release. As a consequence, $A_L(t)$ also sweeps the electron momentum near its zero crossings. This laser-induced sweep is positive (negative) at the positive (negative) slope of $\Delta p(t)$, respectively. Depending on its sign, it increases or decreases the initial sweep of photoelectron momentum imposed by the chirp of the ionizing attosecond *XUV* pulse. This, in turn, gives rise to a broadening or narrowing of the corresponding final momentum (energy) distribution (streak image), respectively, which can be approximated at moderate streaking intensities as $\Delta E \sim 2ep(t_0)A_L(t_0)$, where $p(t_0)$ represents the electron momentum and $A_L(t_0)$ the vector field amplitude of the streaking laser field at time t_0 of its birth. Hence, a negatively-chirped pulse (taken in the example considered in Fig. 4) results in a streaking spectrogram exhibiting narrower/broader streaked spectra at the positive/negative slope of $\Delta p(t)$, exactly as revealed by Fig. 3(c) and 3(f). Conversely, a positively-chirped pulse is predicted to produce a streaking spectrogram with broader/narrower streaked spectra at the positive/negative slope of $\Delta p(t)$, as displayed by Fig. 3(a) and 3(d).

We can now turn our attention to a quantitative evaluation of the chirp carried by the attosecond *XUV* pulse in the three experiments performed with the three different mirrors. Figure 5 shows the retrieved intensity and *GD* of the attosecond pulses after reflection off the

#138629 - $15.00 USD Received 23 Nov 2010; revised 31 Dec 2010; accepted 3 Jan 2011; published 14 Jan 2011

XUV multilayer and filtering by the transmission filter as evaluated from the photo-electron spectrograms in Fig. 3. The solid black lines in Fig. 5(a)–5(c) show a direct measurement of the *XUV* pulse spectrum at the target after passing the filter and the appropriate mirror. Comparison of the retrieved *XUV* spectra (green dotted lines) with those directly measured photon spectra shows remarkable agreement of the bandwidth, spectral profile and central energy position. This agreement between retrieved and measured spectra highlights the precision with which *XUV* mirrors are designed and manufactured and demonstrates the power of attosecond streaking measurements coupled with the *FROG CRAB* retrieval procedure.

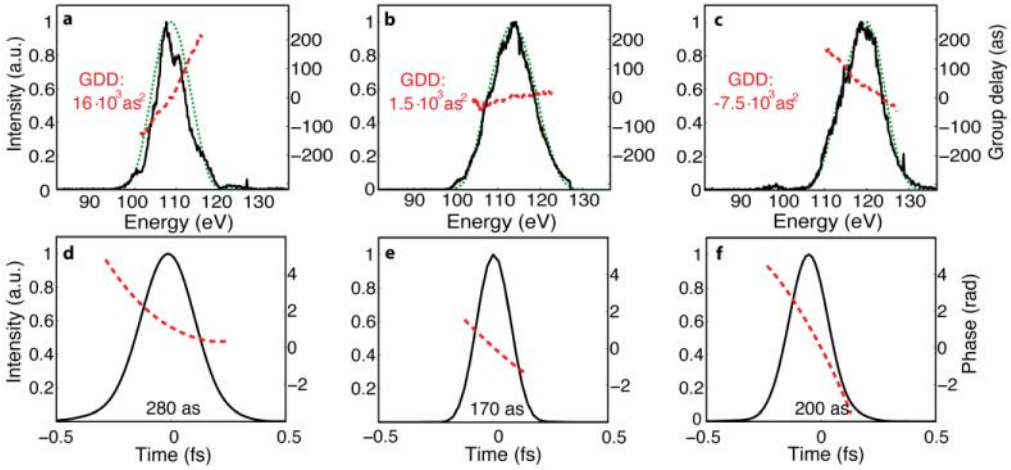

Fig. 5. Retrieved spectral and temporal characteristics of the attosecond *XUV* pulse, upper row and lower row, respectively. Panels (a), (b) and (c) display the intensity spectrum (green dotted line) and group delay (red dashed line) of the attosecond *XUV* pulse reflected off the mirrors described in Fig. 2(a), 2(b), and 2(c), respectively, as retrieved from the measured streaking spectrograms shown in Fig. 3(a), 3(b), and 3(c), respectively. The black full lines depict the corresponding *XUV* spectra measured directly with an *XUV* spectrometer. The evaluated effective group-delay dispersions weighted by the final spectral *XUV* intensity are also shown. Panels (d), (e), (f) show the temporal intensity profile (black line) and temporal phase (red dashed line) retrieved from the streaking spectrograms of Fig. 3(a), 3(b), and 3(c), respectively. The *XUV* pulse duration (full width at intensity half maximum) has been evaluated and is displayed at the bottom of each panel.

Table 1 summarizes the evaluated pulse durations and the *GDD* carried by the reflected pulses, in comparison with the designed *GDD* of the mirrors. Small deviations from the average *GDD* influence the final pulse more if its spectral intensity is high at that energy. Thus, all *GDD* values in Table 1 have been weighted with the spectral profiles $I(\omega)$ of the final pulses for a more meaningful comparison: $GDD_{average}=\int I(\omega)GDD_{\omega}d\omega/\int I(\omega)d\omega$. Comparing the retrieved averaged *GDD* values with the design goals shows an excellent quantitative agreement for two of the mirrors, namely the positive *GDD* (to within 20%), and the near zero *GDD* mirror (to within $\approx 2\text{x}10^3$ as^2, causing negligible pulse broadening in the 100-*as* domain), while the quantitative agreement is compromised by the same layer thickness errors in the negative *GDD* mirror giving rise to the deviations in Fig. 2(c). Note that even thickness deviations on an atomic scale result in significant changes of the mirrors spectral phase response though the reflectance suffers only minor modifications.

#138629 - $15.00 USD Received 23 Nov 2010; revised 31 Dec 2010; accepted 3 Jan 2011; published 14 Jan 2011

Table 1. Comparison of *XUV* mirror designed and *FROG* retrieved pulse parameters*

	Positive *GDD* mirror	Zero *GDD* mirror	Negative *GDD* mirror
GDD design goal	$D_{(+)}$ = **19.5x10^3** *as*^{2}	$D_{(0)}$ = **-0.5x10^3** *as*^{2}	$D_{(-)}$ = **-14x10^3** *as*^{2}
FROG retrieved *GDD*	$D_{(+)}$ = **16x10^3** *as*^{2}	$D_{(0)}$ = **1.5x10^3** *as*^{2}	$D_{(-)}$ = **-7.5x10^3** *as*^{2}
FROG retrieved pulse duration (Fourier limit)	$\tau_{(+)}$ = **280** *as* (200 *as*)	$\tau_{(0)}$ = **170** *as* (165 *as*)	$\tau_{(-)}$ = **200** *as* (175 *as*)

*The average *GDD* values and the appropriate standard deviations are calculated by weighting the calculated and the retrieved discrete *GDD* values with the intensity of the retrieved *XUV* spectrum (see text for a more detailed description). For the positive *GDD* mirror we measure $16x10^3 \pm 4x10^3$ *as*^{2} versus designed $19.5x10^3 \pm 4x10^3$ *as*^{2}, for the zero *GDD* mirror we find $1.5x10^3 \pm 2x10^3$ *as*^{2} versus a design value of $-0.5\ x10^3 \pm 3x10^3$ *as*^{2} and for the negative *GDD* mirror a *GDD* of $-14x10^3 \pm 7.5\ x10^3$ *as*^{2} was designed and $-7.5x10^3 \pm 2x10^3$ *as*^{2} has been retrieved. The lower line shows the retrieved pulse-lengths in comparison to their Fourier limits. It is obvious that the two chirped mirrors broaden the pulse significantly due to the introduced chirp, while there is hardly an effect on the pulse duration by the near zero *GDD* mirror.

Uncertainties in the *XUV* optical constants of the multilayer materials *Mo*, B_4C and *Si* in the 100-130 *eV* energy range may also contribute to the residual discrepancies between design and measurement, with dispersion of the *Pd* filter appearing to be less than $1.5x10^3$ *as*^{2} in the 100-130 *eV* photon energy range. The appearance of a single attosecond pulse in the fringe-less spectrograms (Fig. 3) ensures that our mirror reflectivity peak really coincides with the cut-off spectrum. The near-vanishing chirp of the attosecond pulse filtered from the cut-off range of the high-harmonic spectrum and reflected by the near-zero-*GDD* mirror (b) at the same time validates theoretical considerations that predict the attochirp to be negligible in the cut-off range [32,12]. Finally the good agreement between the retrieved *GDD* values of the produced attosecond pulses and the designed mirror dispersion confirms that the chirp of the attosecond pulse is mainly affected by the mirror, while the intrinsic chirp of the high harmonic generation and the additional filter play subordinate roles.

3. Conclusions

In summary, we have demonstrated control of the chirp and temporal profile of isolated attosecond *XUV* pulses with non-periodic multilayer mirrors in an energy range above 100 *eV*. This technique can be extended to third and higher order phase term treatment as well and is applicable to any spectral range were high reflecting multilayer mirrors are producible, it is important to mention that this range by far exceeds the photon energy range accessible with contemporary high-harmonic-sources. Precision control of the characteristics of attosecond pulses adds an important technical capability to the toolbox of attosecond technology, affording promise for pushing its frontiers to higher temporal resolutions down to the atomic unit of time (24 *as*) and extending coherent control from structural dynamics towards electronic motion in the valence band. High harmonic radiation contains, due to its generation process, intrinsically an essential amount of chirp in a spectral range out of the cut-off region. Precise dispersion control of attosecond pulses could allow us to push the limits to even shorter Fourier-limited pulses, taking spectral bandwidth exceeding the cut-off range and thus entering this temporal regime. Moreover, control over electronic motion in photo-ionization by chirped few-cycle attosecond pulses was recently predicted in a theoretical work by Peng et al. [35]. Furthermore important insight into fundamental electronic structures as the quantum phase can be gained from chirp analyses in electronic states via *XUV* streaking [36]. Absolute control of the chirp of an attosecond pulse becomes even more interesting when we reach the regime of nonlinear processes in the *XUV* range, where for example coherent control by chirped pulses could be achieved. Future seeding of free electron lasers (*FEL*) in the *XUV* by coherent High Harmonic radiation allows for controlling the spectral and temporal *FEL* pulse output with sufficiently high photon numbers [37] and thus requires precise control over the spectral seed chirp as can be provided by the multilayer mirrors described in this paper.

#138629 - $15.00 USD Received 23 Nov 2010; revised 31 Dec 2010; accepted 3 Jan 2011; published 14 Jan 2011

Acknowledgements

This work was supported by the DFG Excellence Cluster "Munich Centre for Advanced Photonics" (MAP). R.K. acknowledges funding from the Sofja Kovalevskaja Award of the Alexander von Humboldt Foundation and an ERC Starting Grant.

#138629 - $15.00 USD Received 23 Nov 2010; revised 31 Dec 2010; accepted 3 Jan 2011; published 14 Jan 2011